A numerical study on local web buckling behaviour of stainless steel coped beams

Mingyuan Zhang[1], Yuchen Song[2], *Ke Ke[3] and Michael C.H. Yam[4]

[1), 2),4)] *Department of Building and Real Estate, The Hong Kong Polytechnic University, Hong Kong SAR, China*
[3)] *School of Civil Engineering, Chongqing University, Chongqing, China*
[4)] *Chinese National Engineering Research Centre for Steel Construction (Hong Kong Branch), The Hong Kong Polytechnic University, Hong Kong SAR, China*
[1)] *ming-yuan.zhang@polyu.edu.hk*
[3)] *ke.ke@cqu.edu.cn*

ABSTRACT

Stainless steel structural members are being increasingly used in steel construction owing to the excellent corrosion resistance and aesthetic appeal. For coped steel beams that are typically encountered in connections between primary and secondary members, the nonlinear stress-strain behaviour of stainless steel may lead to different local web buckling behaviour of coped beams compared with their carbon steel counterparts. To this concern, this paper presents a preliminary numerical study on the local web buckling (LWB) behaviour of stainless steel coped beams. Finite element models are firstly developed and validated against test results from previous studies. A parametric analysis is then conducted covering different parameters including material property, web slenderness, cope details (i.e., cope length and cope depth). According to the numerical results, the failure modes of all the models at the ultimate load are dominated by local web buckling with significant out-of-plane deflection. Compared with carbon steel models that are assigned with identical yield strength and elastic modulus, the 304L stainless steel models exhibit consistently lower ultimate resistances. This should be due to the earlier initiation of nonlinear stress-strain behaviour in 304L stainless steel with a gradual reduction of secant modulus below the yield strength, which eventually leads to lower buckling and ultimate loads of stainless steel coped beams compared with their carbon steel counterparts. The ultimate resistance decreases with the increase of web slenderness ratios and cope lengths and depths for both 304L stainless steel and carbon steel coped beams. Moreover, pronounced post-buckling behaviour is observed in models with more slender webs and greater cope lengths and cope depths. The results obtained from the numerical analysis are also compared with the predictions of two existing design methods. The two methods are found to provide less conservative

---

[1)] Research Assistant
[2)] PhD, Postdoctoral Fellow
[3)] PhD, Professor
[4)] PhD, Professor, Head of Department

predictions for 304L stainless coped beams.

1. INTRODUCTION

Beam coping is widely adopted for the design of steel joints to achieve identical elevations for flanges at the intersection of primary beams and secondary beams. The coped region of a beam is susceptible to local web buckling failure due to the removal of one or both flanges and part of the web. A number of studies have been carried out to examine the local web buckling (LWB) behaviour and resistance of coped beams. Cheng et al. (1984) carried out a systematic study including tests and numerical analyses on the LWB behaviour and resistance of coped beams, and a design method was developed based on a plate buckling model. Yam et al. (2003) re-examined the buckling mechanism of the coped region for single-coped I beams, and proposed an alternative plate shear buckling model. Yam's model showed better agreement with the test results compared with Cheng's method. Recently, Ke et al. (2018) and Yam et al. (2019) investigated the LWB behaviour and resistance of single-coped beams with slender webs, and a pronounced post-buckling behaviour was found for slender webs. Furthermore, a modified design method accounting for the post-buckling mechanism was proposed by Yam et al. (2019) for single-coped beams with slender web. It is noted that the emphases of the studies mentioned above were confined to carbon steel coped beams.

In recent few decades, stainless steel structural members are being increasingly used in steel construction owing to the excellent corrosion resistance and aesthetic appeal. In many cases, coping of stainless steel beams will be inevitable when they are connected to primary structural members. Research on stainless steel bolted connections (Bouchaïr et al. 2008) showed that the failure of the connections occurred at large deformations owing to the great ductility and stain hardening capacity of stainless steel. Moreover, the stainless steel-concrete composite beam-to-column connections investigated by Song et al. (2019) exhibited significant rotation capacity and remarkable enhancement of post-limit moment at large deformations. Considering the unique mechanical characteristics of stainless steel, especially the nonlinear stress-strain behaviour below the yield strength, the LWB behaviour of stainless steel coped beams may be different from their carbon steel counterparts. However, up to date there is no available research nor specific design provisions on stainless steel coped beams, which necessitates further investigations in this field.

This paper presents a preliminary numerical study on the local web buckling (LWB) behaviour of stainless steel coped beams. Finite element models are firstly developed and validated against test results from previous studies. A parametric analysis is then conducted covering different parameters including material property, web slenderness, cope details (i.e., cope length and cope depth). The results obtained from the numerical analysis are also compared with the predictions of various design methods. Finally, comments and recommendations are provided for the design of stainless steel coped beams against local web buckling.

2. NUMERICAL MODELLING

Numerical models were established utilising the commercial finite element (FE) analysis software ABAQUS to investigate the LWB behaviour of stainless steel coped beams. To validate the modelling technique, four test specimens of coped I beams fabricated with hot-rolled steel plates reported in the literature were simulated, including two specimens with compact webs (Yam et al. 2003) and another two specimens with slender webs (Ke et al. 2018). Design details of these four specimens are illustrated in Fig.1 and summarised in Table 1. The material properties obtained from the coupon tests in the literature are listed in Table 2.
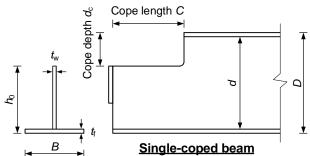

Fig. 1 Illustration of test specimens in the literature (Ke et al. 2018)

Table 1 Detailed information of the four specimens in the literature

Literature	No	Specimen code	D (mm)	B (mm)	t_w (mm)	t_f (mm)	C (mm)	d_c (mm)	R_{test} (kN)	R_{test}/R_{FE}
Ke et al. (2018)	1	C300dc120	600	150	3.82	8	300	120	60.7	1.06
	2	C600dc60	600	150	3.82	8	600	60	40.4	1.04
Yam et al. (2003)	3	406d005	398	142	6.14	8.6	342.9	19.9	165.9	0.96
	4	406d03	398	142	6.14	8.6	342.9	119.4	111.9	1.04

Table 2 Material properties in the literature used for FE models

Literature	Steel grade	Yield strength (MPa)	Ultimate strength (MPa)	Young's modulus (GPa)
Ke et al. (2018)	S355	348	481	194
Yam et al. (2003)	-	343	-	217
Song et al. (2022)	304L	251	625	188

Four-node shell elements with reduced integration (S4R) were employed for the simulation of coped beams. An overall mesh size of 30 mm was adopted for the models and in the coped region, a smaller mesh size of 10 mm was used to enhance the precision of the numerical results. The material property of carbon steel used for the numerical models was simulated using an isotropic elastic-plastic model following von Mises yield criterion. As for the simulation of the welds among the plate components, the 'merge' strategy in ABAQUS was utilized in view of the negligible stress at the weld as observed by Ke et al. (2018). The boundary condition of the end plate was modelled employing an idealised pinned connection constraint that all the translation displacement were restrained (i.e., U1 = U2 = U3 = 0) at the bolt holes. Fig. 2 presents an overview of a typical coped beam model.

The numerical analysis of coped beams was performed via two steps. The first step was an Eigenvalue analysis to obtain the fundamental elastic buckling mode. Then, a nonlinear Riks analysis was conducted in the second step to simulate the nonlinear buckling behaviour of coped beams. The shape of the initial geometric imperfection introduced in the second step is consistent with the first buckling mode obtained in the first step. The amplitude of the initial geometric imperfection was in accordance with that adopted in the literature, which is $0.1\,t_w$ for the two specimens in Ke et al. (2018), and 1 and 0.2 mm respectively for specimens 406d005 and 406d03 tested by Yam et al. (2003).

Fig.2 Overview of a typical coped beam model

The load-deflection curves and failure modes of the specimens were output from the numerical analysis and compared with the test results from the literature (see Fig. 3). Generally, the numerical curves and failure modes agree satisfactorily with the tested results. Moreover, according to the tested-to-predicted ultimate reaction ratios (R_{test}/R_{FE}) listed in Table 1, the discrepancy in the ultimate reaction between the numerical and test results was insignificant, ranging from 4% to 6% for the four specimens.
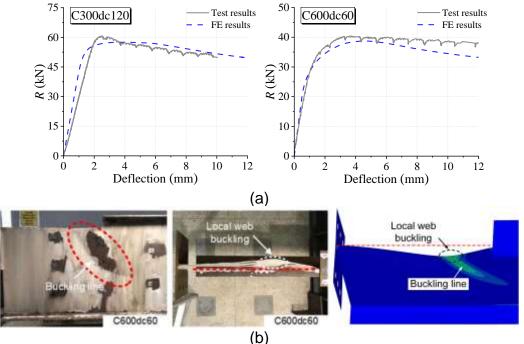

(a)

(b)

Fig. 3 Comparison of numerical and test results: (a) load-deflection curves and (b) failure mode

3. PARAMETRIC ANALYSIS

Utilizing the validated FE models, a parametric analysis covering the variations of material property, web slenderness ratio (d/t_w) and cope details (i.e., cope length and coped depth) was performed to investigate the LWB behaviour of stainless steel coped beams. A total of 21 models were designed by combining the variables mentioned above, and the design details of the models are summarized in Table 3. In particular, two types of steel material, S355 carbon steel and 304L stainless steel, were preliminarily considered in the analysis, dividing the models into two groups (Group A and B). The material properties of S355 steel and 304L stainless steel used in the analysis were identical to that provided by Ke et al. (2018) and Song et al. (2022), respectively, which are listed in Table 2. Three beam depths (D) of 300, 500 and 700 mm were adopted for the I-section beams with the beam width, flange and web thickness of all the models being consistently 150, 8 and 6 mm, hence producing a variation of web slenderness ratio (47.3, 80.7 and 114.0). According to Eurocode 3 (2005 and 2015), the designed three web slenderness ratios classify the I-beam section into Class 1, Class 3 and Class 4 cross-sections, respectively. In addition, three different ratios of cope length to beam depth (C/D) including 0.50, 0.75 and 1.00, accompanied by three ratios of cope depth to beam depth (d_c/D), namely 0.10, 0.15 and 0.20 were considered in the analysis. Note that in the current analysis, the amplitude of initial imperfection was taken as $0.1\,t_w$ for all the models, in consistence with that adopted by Ke et al. (2018). The beam span of the models was designed as 2650 mm, and the distance from the end plate to the loading point was set as $2D$ to mitigate the impact of load concentration on the stress distribution within the coped region.

Table 3 Design details of parametric models

No	Model	Material	D (mm)	B (mm)	t_f (mm)	t_w (mm)	d/t_w	C/D	d_c/D
1	A/D1/C05dc01		300				47.3	0.50	0.10
2	A/D1/C10dc02		300				47.3	1.00	0.20
3	A/D2/C05dc01	S355 steel	500	150	8	6	80.7	0.50	0.10
4	A/D2/C10dc02		500				80.7	1.00	0.20
5	A/D3/C05dc01		700				114.0	0.50	0.10
6	A/D3/C10dc02		700				114.0	1.00	0.20
1	B/D1/C05dc01		300				47.3	0.50	0.10
2	B/D1/C05dc015		300				47.3	0.50	0.15
3	B/D1/C05dc02		300				47.3	0.50	0.20
4	B/D1/C075dc02		300				47.3	0.75	0.20
5	B/D1/C10dc02	304L stainless steel	300				47.3	1.00	0.20
6	B/D2/C05dc01		500	150	8	6	80.7	0.50	0.10
7	B/D2/C05dc015		500				80.7	0.50	0.15
8	B/D2/C05dc02		500				80.7	0.50	0.20
9	B/D2/C075dc02		500				80.7	0.75	0.20
10	B/D2/C10dc02		500				80.7	1.00	0.20
11	B/D3/C05dc01		700				114.0	0.50	0.10

12	B/D3/C05dc015	700		114.0	0.50	0.15
13	B/D3/C05dc02	700		114.0	0.50	0.20
14	B/D3/C075dc02	700		114.0	0.75	0.20
15	B/D3/C10dc02	700		114.0	1.00	0.20

3.1 General failure mode and load-deflection curves

Fig. 4 presents the typical failure mode of the FE models at the ultimate load. Significant out-of-plane (U1 direction) deflections (Fig. 4(a)) were observed within the coped region, exhibiting a local web buckling failure. As can be seen from Fig. 4, the out-of-plane deflection at the ultimate load was increased with the increase of web slenderness ratio, accompanied by more extensive yielding area. According to the PEEQ (equivalent plastic strain) contours shown in Fig. 4(b), the plastic strains in 304L stainless steel models have lower magnitude but more extensive distributions than those of S355 carbon steel counterparts at the ultimate load.
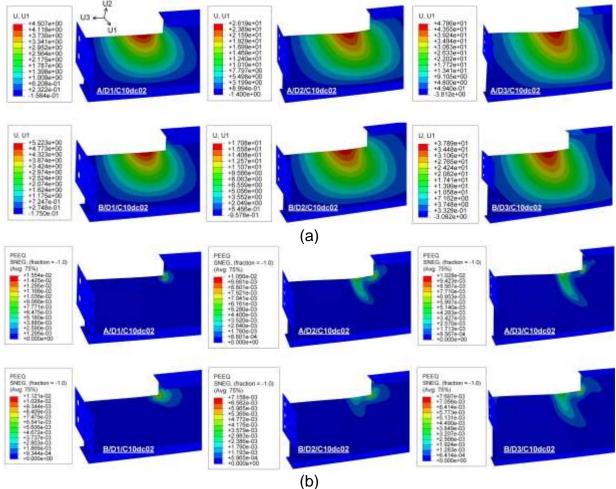

(a)

(b)

Fig. 4 Typical failure mode of FE models at the ultimate load: (a) contours of out-of-plane deflection; (b) contours of PEEQ.

The obtained load (reaction at the end plate calculated by the applied concentrated load minus the reaction at the far beam end) versus deflection (in-plane deflection at the load point) curves are shown in Fig. 5. Elastic buckling resistance (R_{EG}) obtained from

the Eigenvalue analysis is also indicated in Fig. 5. For models with the ultimate resistance (R_u) larger than R_{EG}, the R_{EG} values were depicted by a horizonal dashed line, while the R_{EG} values of models with R_u smaller than R_{EG} were not displayed. It can be seen from Fig. 5 that the R_u of models with compact webs and smaller cope lengths and depths were less than R_{EG}, due to an inelastic local web buckling failure behaviour by accounting for the material and geometry nonlinearity. However, for three models with slender webs and greater cope lengths and depths, the R_u were larger than R_{EG}, indicating the development of post-buckling behaviour after the initial local buckling.
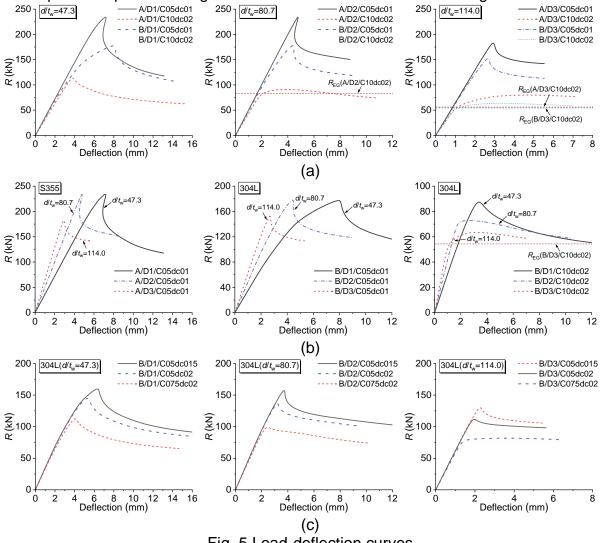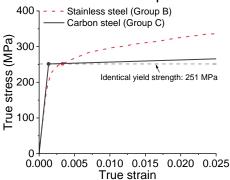

(a)

(b)

(c)

Fig. 5 Load-deflection curves

3.2 Effect of material property

It was observed from Fig. 5(a) that the ultimate resistance of 304L stainless steel coped beam models (belongs to Group B) was much lower than that of S355 carbon steel counterparts (Group A) with identical cope details and web slenderness. As the yield strengths and stress-strain relationships of the two groups of models were both varied, it is hard to determine which was the crucially influential factor attributed to this discrepancy. To further investigate this, an additional analysis including six models

adopting a carbon steel with identical yield strength (f_y = 251 MPa) and elastic modulus (E = 188 GPa) to 304L stainless steel was conducted, and these models are designated as Group C. Fig. 6 shows the stress-strain curves of the two materials. The comparison of load versus deflection curves between Group B and C models are presented in Fig. 7, and the R_{EG} of the models is also indicated as presented in Fig. 5.

As can be seen from Fig 7, although the yield strengths of the two groups of models (Group B and C) are identical, the ultimate resistance of 304L stainless steel models (Group B) was still consistently lower than that of carbon steel models (Group C). The load-deflection behaviour within the elastic stage and R_{EG} value of the two materials of models were found to be consistent owing to an identical initial elastic stiffness. However, earlier initiation of nonlinear behaviour was observed in 304L stainless steel models. Subsequently, the (in-plane) deflections of 304L stainless steel models were much greater than those of their carbon steel counterparts with identical yield strength at the same load. At the ultimate load, the deflections of 304L stainless steel models exceeded or approached to those of their carbon steel counterparts with identical yield strength.
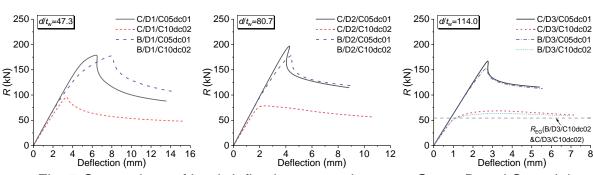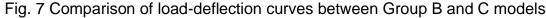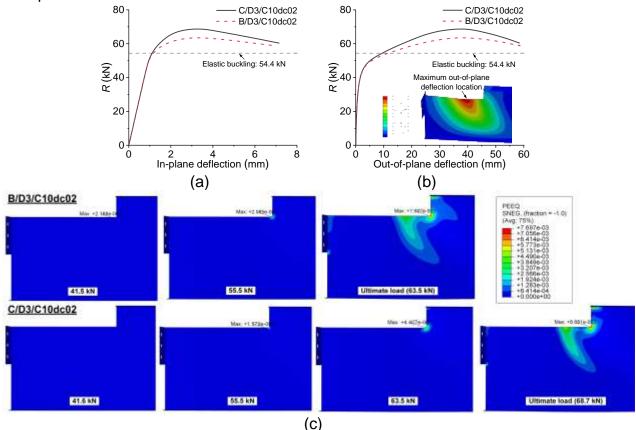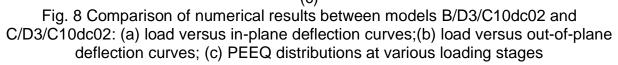

Fig. 6 Stress-strain curves of 304L stainless steel and carbon steel

Fig. 7 Comparison of load-deflection curves between Group B and C models

In order to further confirm this, Fig. 8 additionally presents the comparison of load versus in-plane and out-of-plane deflection (at the maximum out-of-plane deflection location as shown in Fig. 8(b)) curves of models B/D3/C10dc02 and C/D3/C10dc02. The PEEQ distributions are also displayed for the two models corresponding to several critical loading stages. As shown in Fig. 8(c), inelastic strain was only observed in model B/D3/C10dc02 but not found in model C/D3/C10dc02 at a load of 41.5 kN, which is due to the earlier initiation of material nonlinearity for 304L stainless steel. Moreover, at loads of 55.5 and 63.5 kN (ultimate load of model B/D3/C10dc02), the maximum inelastic strains of model B/D3/C10dc02 were greater than that of model C/D3/C10dc02. At the

same time, the in-plane and out-of-plane deflections of model B/D3/C10dc02 were also greater (see Fig. 8(a) and Fig. 8(b)). Although the ultimate load of model B/D3/C10dc02 was comparatively lower, the models B/D3/C10dc02 and C/D3/C10dc02 achieved similar in-plane deflections of 3.25 and 3.26 mm, and out-of-plane deflections of 37.9 and 37.5 mm, respectively. Therefore, it is preliminary concluded that the difference in the ultimate resistance of 304L stainless steel and carbon steel with identical yield strength models was due to the earlier initiation of nonlinear stress-strain behaviour of 304L stainless steel. That is, compared with carbon steel with roughly consistent stiffness below the yield strength, the nonlinear stress-strain behaviour of 304L stainless steel with gradually deteriorated stiffness (Fig. 6) leads to a reduction of buckling load and ultimate resistance of coped beams.

(a) (b)

(c)

Fig. 8 Comparison of numerical results between models B/D3/C10dc02 and C/D3/C10dc02: (a) load versus in-plane deflection curves;(b) load versus out-of-plane deflection curves; (c) PEEQ distributions at various loading stages

3.3 Effects of web slenderness ratios and cope details

As shown in Fig. 5(b), the ultimate resistance decreases with the increase of web slenderness ratio for both 304L stainless and S355 carbon steel coped beam models. This indicates that coped beams with more slender web are more susceptible to local web buckling failure. In particular, a reduction of 14% in the ultimate resistance was characterised when the web slenderness ratio increased from 47.3 to 114.0 for 304L stainless steel models. In current analysis, two models of A/D3/C10dc02 and B/D3/C10dc02 with the most slender web (d/t_w = 114.0) reached a ultimate resistance

greater than the elastic buckling resistance (see Fig. 5(a)), indicating that the post-buckling behaviour got more pronounced for models with more slender web and greater cope lengths and depths.

Fig. 5(c) and Fig. 9 illustrate the effects of cope details (i.e., cope length and cope depth) on the LWB behaviour of 304L stainless steel coped beams. As can be seen from Fig. 5(c), the ultimate resistance (R_u) was significantly decreased, and reached at a reduced deflection when C/D and d_c/D ratios increased. Fig. 9 plots the correlation of R_u with C/D and d_c/D ratios. A considerable reduction in R_u was found as the C/D ratio increased, which may be due to the increase of cope length causing a longer web region prone to buckle. In the current analysis, when the C/D ratio increased from 0.50 to 1.00, a maximum decrease of 47% was observed for 304L stainless steel models with d/t_w ratio of 80.7 and d_c/D ratio of 0.20. As for the influence of the d_c/D ratio, an average decrease of 23% in R_u was obtained for three different web slenderness ratios of 304L stainless steel coped beams by ranging the d_c/D ratio from 0.10 to 0.20. The reduction in R_u could be due to the reduced elastic section modulus of the coped web section (T-section) leading to an increase of the compressive stress along the top edge of the web. Generally, these analytical results are in consistence with the findings characterised from previous studies on coped beams made from carbon steel, which can be found in Ke et al. (2018).
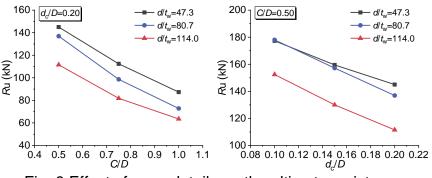

Fig. 9 Effect of cope details on the ultimate resistance

4. EVALUATION OF CURRENT DESIGN EQUATIONS

In this section, the ultimate resistance obtained from the numerical analysis was compared with that predicted by the design method developed by Yam et al. (2003) and Yam et al. (2019), in order to evaluate the adequacy of these methods to calculate the LWB resistance of stainless steel coped beams.

According to Yam's equations (2003), the buckling failure of a coped beam is determined by the critical shear stress τ_{cr}, which is calculated by:

$$\tau_{cr} = k_s \frac{\pi^2 E}{12(1-v^2)} \left(\frac{t_w}{h_0}\right)^2 \tag{1}$$

where k_s is the shear buckling coefficient calculated as:

$$k_s = a\left(\frac{h_0}{C}\right)^b \tag{2}$$

$$a = 1.38 - 1.79\frac{d_c}{D} \tag{3}$$

$$b = 3.64\left(\frac{d_c}{D}\right)^2 - 3.36\frac{d_c}{D} + 1.55 \tag{4}$$

the critical reaction (R_{cr}) is calculated by $R_{cr}=\tau_{cr}t_wh_0$, provided that τ_{cr} is less than the shear yielding stress (f_{yv}). If τ_{cr} is greater than f_{yv}, the reaction is determined by $R_{vy}=f_{yv}h_0t_w$. Moreover, the reaction dominated by the bending yielding (R_y) is calculated according to $R_y=f_yS_{Tee}/C$, where S_{Tee} is the elastic section modulus of the T section. Then, the ultimate resistance (R_{Yam1}) is taken as the lowest value among R_{cr}, R_{vy} and R_y.

For predicting the LWB resistance of single-coped beams with slender webs, Yam et al. (2019) proposed an updated critical shear stress τ_{cr} by modifying the coefficient to calculate k_s in Eq. (2) as follows:

$$a=a_1\left(\frac{d_c}{D}\right)+a_2 \tag{5}$$

$$b=a_3\left(\frac{d_c}{D}\right)^2+a_4\left(\frac{d_c}{D}\right)+a_5 \tag{6}$$

where a_1, a_2, a_3, a_4 and a_5 are coefficients determined by a curve fitting procedure. It is recommended that $a_1=-2.70$, $a_2=1.73$, $a_3=5.50$, $a_4=-4.35$, and $a_5 = 2.00$.

In addition, a modification factor (W) considering the effect of web slenderness and cope details is proposed:

$$W=\left(c_1\frac{D}{100t_w}+c_2\right)\left(\frac{h_0}{c}\right)+\left(c_3\frac{D}{100t_w}+c_4\right) \tag{7}$$

where coefficients c_1, c_2, c_3 and c_4 were determined by:

$$c_1=6.60\left(\frac{c}{D}\right)^2-8.72\left(\frac{c}{D}\right)+1.47 \tag{8}$$

$$c_2=-4.33\left(\frac{c}{D}\right)^2+3.70\left(\frac{c}{D}\right)+0.14 \tag{9}$$

$$c_3=-3.00\left(\frac{c}{D}\right)^2+2.50\left(\frac{c}{D}\right)+1.91 \tag{10}$$

$$c_4=-0.61\left(\frac{c}{D}\right)^2+4.40\left(\frac{c}{D}\right)-3.08 \tag{11}$$

Note that the modification factor Q_v proposed by Yam et al. (2019) to account for the influences of the rotational restraint of the end-plate connection is neglected in current analysis, therefore, the design resistance of a single-coped beam with slender web (R_{Mo}) is given by:

$$R_{Mo}=WR_{cr} \tag{12}$$

It is worth mentioning that Yam's method (2019) is limited to coped beams with the web slenderness ratio (D/t_w) ranging from 100 to 150, therefore in the current analysis, it was only adopted for modes with d/t_w ratio of 114.0. Table 4 summarizes the comparison of the numerical results (R_{FE}) and predictions given by the Yam's method 2003 (R_{Yam1}) and Yam's method 2019 (R_{Yam2}). The FE-to-predicted ratios determined by elastic critical resistance (R_{cr} and R_{Mo}) of stainless steel coped beams appeared to be lower than that of carbon steel counterparts according to both methods. The FE-to-predicted ratios of several 304L stainless steel coped beams given by both methods were less than one, indicating unconservative predictions of the methods. In particular, the mean FE-to-predicted ratios of carbon steel coped beams according to Yam's method (2003) and Yam's method (2019) were 1.12 with the CoV of 0.137 and 0.89 with the CoV of 0.064, respectively. Comparatively, for 304L stainless steel coped beams, the mean FE-to-predicted ratio obtained from Yam's method (2003) and Yam's method (2019) were 0.99 with the CoV of 0.098 and 0.77 with the CoV of 0.018. This discrepancy could mainly be due to the fact that both methods were derived based on the concept of elastic buckling with a consistent elastic modulus. However, according to the current analysis, the 304L

stainless steel displayed a nonlinear stress-strain behaviour with degradation of stiffness prior to the yield strength (Fig. 6), which leads to a lower ultimate resistance of stainless steel coped beams compared with their carbon steel counterparts. Therefore, the two design methods that assume a consistent elastic modulus may not be applicable to 304L stainless coped beams.

To improve the accuracy of predicting the LWB resistance of stainless steel coped beams, it is preliminarily recommended that a modified design method based on the inelastic buckling concept may be developed, accounting for the nonlinear stress-strain behaviour of stainless steel below the yield strength.

Table 4 Comparisons between numerical results and predictions by design equations

No	Model	R_u (kN)	R_y (kN)	R_{vy} (kN)	Yam's method 2003		Yam's method 2019	
					R_{cr} (kN)	R_u/R_{Yam1}	R_{Mo} (kN)	R_u/R_{Yam2}
1	A/D1/C05dc01	234.1	262.1	325.3	352.8	<u>0.89</u>	-	-
2	A/D1/C10dc02	113.4	105.0	289.1	128.9	<u>1.08</u>	-	-
3	A/D2/C05dc01	234.2	406.5	542.1	211.7	1.11	-	-
4	A/D2/C10dc02	90.8	163.5	481.9	77.3	1.17	-	-
5	A/D3/C05dc01	182.6	539.7	759.0	151.2	1.21	194.2	0.94
6	A/D3/C10dc02	79.9	217.3	674.7	55.2	1.45	85.3	0.94
7	C/D1/C05dc01	178.8	189.3	235.0	352.8	<u>0.94</u>	-	-
8	C/D1/C10dc02	95.0	75.8	208.8	128.9	<u>1.25</u>	-	-
9	C/D2/C05dc01	196.8	293.6	391.6	211.7	0.93	-	-
10	C/D2/C10dc02	78.5	118.1	348.1	77.3	1.02	-	-
11	C/D3/C05dc01	167.0	389.8	548.2	151.2	1.10	194.2	0.86
12	C/D3/C10dc02	68.7	156.9	487.3	55.2	1.24	85.3	0.81
					Mean	1.12	Mean	0.89
					CoV	0.137	CoV	0.064
1	B/D1/C05dc01	177.3	189.3	235.0	352.8	<u>0.94</u>	-	-
2	B/D1/C05dc015	159.5	170.0	221.9	301.6	<u>0.94</u>	-	-
3	B/D1/C05dc02	145.0	151.7	208.8	262.0	<u>0.96</u>	-	-
4	B/D1/C075dc02	112.4	101.1	208.8	173.0	<u>1.11</u>	-	-
5	B/D1/C10dc02	87.3	75.8	208.8	128.9	<u>1.15</u>	-	-
6	B/D2/C05dc01	178.0	293.6	391.6	211.7	0.84	-	-
7	B/D2/C05dc015	157.2	264.2	369.8	181.0	0.87	-	-
8	B/D2/C05dc02	136.9	236.2	348.1	157.2	0.87	-	-
9	B/D2/C075dc02	98.6	157.4	348.1	103.8	0.95	-	-
10	B/D2/C10dc02	72.8	118.1	348.1	77.3	0.94	-	-
11	B/D3/C05dc01	152.4	389.8	548.2	151.2	1.01	194.2	0.79
12	B/D3/C05dc015	130.0	350.9	517.8	129.3	1.01	167.6	0.78
13	B/D3/C05dc02	111.5	313.9	487.3	112.3	0.99	146.9	0.76
14	B/D3/C075dc02	81.8	209.2	487.3	74.1	1.10	106.2	0.77
15	B/D3/C10dc02	63.5	156.9	487.3	55.2	1.15	85.3	0.74
					Mean	0.99	Mean	0.77
					CoV	0.098	CoV	0.018

Notes: The predictions dominated by bending or shear yielding (R_y or R_{vy}) were underlined.

5. CONCLUSIONS

This paper presented a preliminary numerical study on the local web buckling (LWB) behaviour of stainless steel coped beams. Finite element models were firstly developed and validated against test results from previous studies. A parametric analysis was then conducted covering different parameters including material property, web slenderness, cope details (i.e., cope length and cope depth). The ultimate resistance of 304L stainless steel coped beams appeared to be much lower than that of S355 carbon steel counterparts with identical cope details and web slenderness. According to an additional analysis adopting carbon steel with identical yield strength to 304L stainless steel, it was found that the ultimate resistances of stainless steel coped beams were still lower than those of carbon steel coped beams with the same yield strength. This is due to the earlier initiation of nonlinear stress-strain behaviour (below the yield strength) in 304L stainless steel, which leads to a reduction of buckling load and consequently reduced ultimate resistance. The ultimate resistance decreased with increasing web slenderness ratio for both 304L stainless steel and carbon steel coped beams. Pronounced post-buckling mechanism was observed in models with more slender webs and greater cope lengths and cope depths through comparing the ultimate resistance with the elastic buckling load. A considerable decrease in the ultimate resistance was found when the cope lengths and cope depths increased.

Based on the numerical results, the adequacy of two design methods for calculating the LWB resistance of stainless steel coped beams was assessed. In general, the two methods gave less conservative predictions for stainless steel coped beams. Due to the nonlinear stress-strain behaviour of 304 stainless steel with degradation of stiffness prior to the yield strength, the two design methods that assume a consistent elastic modulus may not be applicable to 304L stainless coped beams. It is preliminarily recommended that a modified design method based on the inelastic buckling concept may be developed, accounting for the nonlinear stress-strain behaviour of stainless steel.

ACKNOWLEDGEMENT

REFERENCES

Cheng, J.J.R., Yura, J.A. and Johnson, C.P. (1984), ''Design and behaviour of coped beams'', Phil M. Ferguson Structural Engineering Laboratory Rep. No. 84-1, Univ. of Texas at Austin, Austine, Tex.

Yam, M.C.H., Lam, A.C.C., Iu, V.P. and Cheng, J.J.R. (2003), "Local web buckling strength of coped steel I beams", *J. Struct. Eng.*, **129**(1), 3-11.

Ke, K., Yam, M.C.H., Lam, A.C. and Chung, K. F. (2018), "Local web buckling of single coped beam connections with slender web", *J. Constr. Steel. Res.*, **150**, 543-555.

Yam, M.C.H., Ke, K., Lam, A.C. and Zhao, Q. (2019), "Performance of single-coped beam with slender web and quantification of local web buckling strength", *Thin. Wall. Struct.*, **144**, 106355.

Bouchaïr, A., Averseng, J., Abidelah, A. (2008), "Analysis of the behaviour of stainless steel bolted connections", *J. Constr. Steel. Res.*, **64**(11), 1264-1274.

Song, Y., Uy, B., Wang, J. (2019), "Numerical analysis of stainless steel-concrete composite beam-to-column joints with bolted flush endplates", *Steel. Compos. Struct.*, **33**(1), 143-162.

Song, Y., Uy, B., Li, D., Wang, J. (2022), "Ultimate behaviour and rotation capacity of stainless steel end-plate connections", *Steel. Compos. Struct.*, **42**(4), 569-590.

CEN EN 1993-1-8 (2005), Eurocode 3: Design of Steel Structures, Part 1-8: Design of Joints, Comité Européen de Normalisation, Brussels, Belgium.

CEN EN 1993-1-4:2006+A1 (2015), Eurocode 3: Design of Steel Structures, Part 1-4: General Rules-Supplementary Rules for Stainless Steels, Comité Européen de Normalisation, Brussels, Belgium.